Available online at www.sciencedirect.com

ScienceDirect

Procedia Structural Integrity 2 (2016) 1991–1998

Structural Integrity Procedia

www.elsevier.com/locate/procedia

21st European Conference on Fracture, ECF21, June 20–24, 2016, Catania, Italy

A numerical finite fracture mechanics approach on asymmetric cracks in open-hole plates

P. L. Rosendahl[a,*], P. Weißgraeber[b], N. Stein[a], W. Becker[a]

[a]*Technische Universität Darmstadt, Fachgebiet Strukturmechanik, Franziska-Braun-Str. 7, 64287 Darmstadt, Germany*
[b]*Robert Bosch GmbH, Corporate Research and Advance Engineering, Renningen, Germany*

Abstract

Using an efficient numerical approach, a model rendering the initiation of asymmetric crack patterns in open-hole plates subject to combined tensile and in-plane bending loading is presented. In the framework of finite fracture mechanics a stress and an energy criterion are enforced simultaneously and used as a coupled condition for the formation of cracks of finite size. Using closed-form expressions for the dependence of the stress and energy quantities needed to solve the coupled criterion on the structural and material parameters, only a limited number of linear elastic finite element analyses is required for a comprehensive analysis of the notched plate. The failure load predictions of the presented model are shown to agree well with experimental results and predictions of a cohesive zone model. The finite fracture mechanics approach allows for a study of crack patterns associated to failure.

Keywords: Finite fracture mechanics, asymmetric cracks, brittle fracture, size effect

1. Introduction

Stress raisers such as open-holes or rounded notches can be found in almost any structure. Due to the local stress concentration, they constitute prominent locations for crack initiation. The non-singular nature of the stress field, however, leads to vanishing energy release rates such that classical fracture mechanics concepts as the Griffith criterion (Griffith, 1921) cannot be applied directly. An additional non-physical length parameter as e.g. an existing finite sized crack or internal flaw (Waddoups et al., 1971) needs to be assumed. In order to render size effects, stress based criteria need to be evaluated at a certain distance from the stress concentration as proposed by Whitney and Nuismer (1974). In the framework of finite fracture mechanics (FFM), the need for an empirical length scale can be eliminated. Here, the instantaneous initiation of cracks of finite size is assumed if both, a stress and an energy criterion are satisfied simultaneously. This so-called coupled criterion proposed by Leguillon (2002) requires only the two fundamental material properties strength and fracture toughness to study the onset of brittle fracture. It allows for the assessment of arbitrary crack initiation patterns and provides the finite crack sizes as well as the critical load.

* Corresponding author. Tel.: +49 6151 16-26147, Fax: +49 6151 16-26142
E-mail address: rosendahl@fsm.tu-darmstadt.de (P. L. Rosendahl).

10.1016/j.prostr.2016.06.250

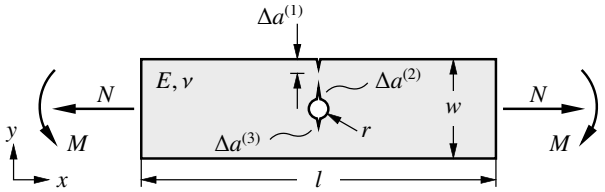

Fig. 1. Open-hole plate subjected to normal force N and in-plane bending loading M. The plate is of width w, length l, unity thickness and has a center hole of radius r. Cracks of the lengths $\Delta a^{(i)}$ are expected to occur. A homogeneous, isotropic material of Young's modulus E and Poisson's ratio ν is assumed.

The coupled criterion has been successfully applied by many researchers in order to investigate cracking of various structural situations such as cracks originating from U-notches (Hebel and Becker, 2008; Andersons et al., 2010; Carpinteri et al., 2012; Cicero et al., 2012), bolted (Catalanotti and Camanho, 2013) or adhesive joints (Weißgraeber and Becker, 2013; Hell et al., 2014; Stein et al., 2015; Carrère et al., 2015), open-holes in composite plates subject to uniaxial tension and compression (Camanho et al., 2012; Martin et al., 2012; Erçin et al., 2013; Romani et al., 2015) and elliptical holes (Weißgraeber et al., 2015). Weißgraeber et al. (2016) give a comprehensive review of the applications of finite fracture mechanics and the coupled criterion.

In real structures uniaxial tension loading is rather a special case. The present work uses a numerical approach in order to extend the application of the coupled criterion to crack initiation at open-holes under more general loading. An arbitrary superposition of tensile and bending loading is considered such that asymmetric crack patterns are expected to occur. The approach includes both limit cases: uniaxial tension and pure bending.

2. Open-hole plate under tensile and bending loading

The present study examines a brittle open-hole plate of unity thickness, width w, length l and a circular center hole of the radius r, as depicted in Fig. 1. Under the combined tensile N and in-plane bending loading M at least one of the three cracks $\Delta a^{(1)}$, $\Delta a^{(2)}$ or $\Delta a^{(3)}$ is expected to emanate.

The chosen numerical approach requires a parametric study of the structural parameters. For an efficient analysis, the use of the parameters introduced in the following proved advantageous. As a measure of the proportion of tensile and bending loading

$$\Lambda = \sqrt{\frac{\Pi^{\mathrm{i}}_{\mathrm{M}}}{\Pi^{\mathrm{i}}_{\mathrm{M}} + \Pi^{\mathrm{i}}_{\mathrm{N}}}}\,, \qquad \Lambda \in [0,1]\,, \tag{1}$$

is defined, where $\Pi^{\mathrm{i}}_{\mathrm{N}}$ denotes the strain energy due to pure tensile loading and $\Pi^{\mathrm{i}}_{\mathrm{M}}$ due to pure in-plane bending, respectively. In order to express Λ in terms of normal force and bending moment, the strain energy of an Euler-Bernoulli-beam is considered. A useful measure for the ratio of tensile and bending loading is obtained, although, of course, the Euler-Bernoulli theory does not apply to the notched section of the beam. The denominator of the newly obtained expression for Λ is used as the total loading parameter P:

$$\Lambda = \frac{M}{\sqrt{M^2 + \frac{w^2}{12}N^2}}\,, \qquad P = \sqrt{M^2 + \frac{w^2}{12}N^2}\,. \tag{2}$$

In subsequent sections, Eq. (2) will be used as the definition of Λ. The two quantities, Λ and P, allow for the characterization of both, the tensile and the bending loading:

$$N = 2\sqrt{3}\frac{P}{w}\sqrt{1-\Lambda^2}\,, \qquad M = \Lambda P\,. \tag{3}$$

The non-dimensional hole size ω, which corresponds to the fraction of hole diameter $2r$ and width w reads

$$\omega = \frac{2r}{w}\,, \qquad \omega \in [0,1)\,. \tag{4}$$

In order to ensure that any disturbance in the stress and displacement fields will decay sufficiently to the ends of the plate where the loads are applied, a constant ratio of length to width

$$\frac{l}{w} = 2(1 + 4\omega) \,, \tag{5}$$

is chosen. This is in accordance to Saint-Vernant's principle. The non-dimensional crack lengths

$$\delta^{(i)} = \frac{2\Delta a^{(i)}}{w(1-\omega)} \,, \qquad 0 \leq \delta^{(i)} \leq 1 \,, \qquad i = 1, 2, 3 \,, \tag{6}$$

are defined as the fraction of the dimensional crack lengths $\Delta a^{(i)}$ and the distance between hole and edges. The additional restriction

$$0 \leq \delta^{(1)} + \delta^{(2)} \leq 1 \,, \tag{7}$$

applies to the sum of the cracks on the bending tension side of the hole (cf. Fig. 1) as they share the same ligament. As discussed in Section 5, the simultaneous appearance of three cracks is observed for only a few, isolated parameter configurations. Therefore, only patterns of two cracks are investigated. The simultaneous initiation of only $\Delta a^{(1)}$ and $\Delta a^{(3)}$ (cf. Fig. 1) is not expected and excluded. The crack pattern for which only cracks at the hole, $\Delta a^{(2)}$ and $\Delta a^{(3)}$, are present is referred to as configuration A. It is typical for pure tension or weak bending. Crack pattern B corresponds to the configuration where the edge crack $\Delta a^{(1)}$ and the crack at the hole on the bending tension side $\Delta a^{(2)}$ emanate. Moreover, since the stress concentration at the hole on the bending tension side dominates for most loading and geometry cases, $\Delta a^{(2)}$ is expected to be present in most crack configuration patterns. It is therefore advantageous to introduce a crack length ratio ψ for both crack configurations, which relates the cracks $\Delta a^{(1)}$ and $\Delta a^{(3)}$ to $\Delta a^{(2)}$:

$$\psi_{\mathrm{A}} = \frac{\delta^{(3)}}{\delta^{(2)} + \delta^{(3)}} = \frac{\Delta a^{(3)}}{\Delta a^{(2)} + \Delta a^{(3)}} \,, \qquad \psi_{\mathrm{A}} \in [0, 1] \,, \tag{8}$$

$$\psi_{\mathrm{B}} = \frac{\delta^{(1)}}{\delta^{(1)} + \delta^{(2)}} = \frac{\Delta a^{(1)}}{\Delta a^{(1)} + \Delta a^{(2)}} \,, \qquad \psi_{\mathrm{B}} \in [0, 1] \,. \tag{9}$$

Both crack length ratios incorporate the limit case of exclusive appearance of $\Delta a^{(2)}$ for $\psi_{\mathrm{A,B}} = 0$. $\psi_{\mathrm{A}} = 1$ corresponds to a sole existence of $\Delta a^{(3)}$ and $\psi_{\mathrm{B}} = 1$ to the sole existence of $\Delta a^{(1)}$.

In total, a set of nine parameters fully describes the plate's geometry, material, loading and possible crack patterns. These are the width w, the relative hole size ω, the load P, the fraction of bending Λ, the non-dimensional crack length $\delta^{(2)}$ and the crack lengths ratio parameters ψ_{A} and ψ_{B} as well as the Young's modulus E and the Poisson's ratio ν.

3. Finite fracture mechanics failure model

In contrast to linear elastic fracture mechanics or pure strength of materials assessments, finite fracture mechanics (FFM) is capable of modeling brittle crack initiation at arbitrary stress concentrations without the need for a non-physical length parameter. The coupled criterion proposed by Leguillon (2002) enforces the simultaneous satisfaction of a stress and an energy criterion

$$F(\sigma_{ij}(\mathbf{x})) \geq \sigma_{\mathrm{c}} \; \forall \; \mathbf{x} \in \Omega(\Delta A) \quad \wedge \quad \bar{\mathcal{G}}(\Delta A) \geq \mathcal{G}_{\mathrm{c}} \,, \tag{10}$$

where $\Omega(\Delta A)$ is the potential crack surface of the finite sized crack and $F(\sigma_{ij}(\mathbf{x}))$ an appropriate equivalent stress function for the structural situation. The incremental energy release rate

$$\bar{\mathcal{G}} = \frac{1}{\Delta A} \int_0^{\Delta A} \mathcal{G}(\tilde{A}) \, \mathrm{d}\tilde{A} = -\frac{\Delta \Pi}{\Delta A} \,, \tag{11}$$

relates the finite change in potential energy $\Delta\Pi$ to the finite crack growth ΔA. For infinitesimal crack growth it reverts to the well known differential energy release rate $\mathcal{G}$. Thus, the incremental energy release rate can be obtained from the

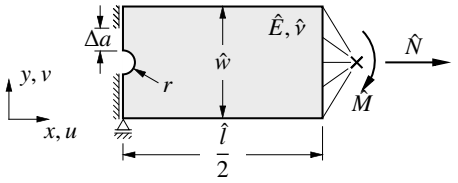

Fig. 2. FEA half-model. Quantities with a hat are constant for all analyses.

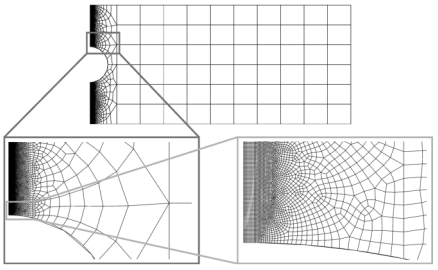

Fig. 3. True to scale rendering of the finite element mesh.

differential energy release rate through integration, see Eq. (11). Using two necessary conditions for crack onset the coupled criterion, Eq. (10), provides the two unknowns, the critical load and the finite crack size – requiring only the two fundamental material properties strength σ_c and toughness $\mathcal{G}_c$. There is no need for empirical length parameters.

For the present plate of unity thickness the finite crack size ΔA reverts to a finite crack length Δa. As depicted in Fig. 1, at least one of three cracks is expected to emanate. The crack configuration can be described using the crack lengths vector

$$\mathbf{\Delta a} = \left[\Delta a^{(1)},\ \Delta a^{(2)},\ \Delta a^{(3)}\right]^{\mathrm{T}} , \tag{12}$$

composed of the three possible crack lengths. The surface of a certain crack pattern is denoted as $\Omega(\mathbf{\Delta a})$. The energy criterion for the initiation of multiple cracks reads

$$\bar{\mathcal{G}}\left(\mathbf{\Delta a}\right) = \frac{-\Delta\Pi}{\Delta a^{(1)} + \Delta a^{(2)} + \Delta a^{(3)}} \geq \mathcal{G}_c , \tag{13}$$

where $\Delta\Pi$ is the difference in total potential energy between the uncracked and cracked configuration. Cracked denotes configurations for which at least one of the three crack lengths $\Delta a^{(i)}$ is non-zero. The original proposal of the coupled criterion (Leguillon, 2002), involves a point-wise stress evaluation. The equivalent stress function is required to exceed the strength on every point of the potential crack surface. Therefore, it will be referred to as point method (PM-FFM). Using the point method yields the coupled criterion for the present problem in the form

$$\sigma_I(y) \geq \sigma_c \ \forall\ y \in \Omega\left(\mathbf{\Delta a}\right) \quad \wedge \quad \bar{\mathcal{G}}\left(\mathbf{\Delta a}\right) \geq \mathcal{G}_c , \tag{14}$$

where σ_I is the maximum principal stress chosen as the equivalent stress function due to the pure mode I crack opening. As an alternative approach Cornetti et al. (2006) suggested to average the equivalent stress function over the finite crack lengths $\Delta a^{(i)}$. This yields the coupled criterion in the form

$$\frac{1}{\Delta a^{(i)}} \int_0^{\Delta a^{(i)}} \sigma_I(\tilde{y})\, \mathrm{d}\tilde{y} \geq \sigma_c \ \forall\ i \in \{1,2,3\} \quad \wedge \quad \bar{\mathcal{G}}\left(\mathbf{\Delta a}\right) \geq \mathcal{G}_c , \tag{15}$$

the so-called line method (FFM-LM).

Since to the authors' knowledge no closed-form analytical solution for the required stress and energy quantities is available, they are extracted from linear elastic finite element analyses using the commercial FE *Abaqus* 6.13 and its *Python* scripting interface. The corresponding FEA model is shown in Fig. 2 and Fig. 3. For a comprehensive analysis of the open-hole plate only the hole size and the crack lengths need to be investigated in a parametric study. The dependencies of the stress and energy quantities on the governing parameters (cf. Fig. 2) can either be given in closed-form or are negligible as shown in the subsequent paragraphs.

Taking advantage of the linear elastic analysis, normal force and bending moment are applied individually in separate analysis steps. The combined stress field is obtained from the superposition of both individual loading cases. Both individual stress fields scale proportionally to the applied loads under the Neumann type loading boundary conditions. Since the governing Navier-Cauchy equations are scale-invariant if the boundary conditions are scaled equally to the equations, dependencies of the stress fields on the plate's width can be obtained easily. The stress field under normal

force loading is inverse proportional to the width whereas the stress field due to in-plane bending loading scales inverse proportional to the square of the width. For arbitrary loading and structure size we obtain the total stresses as

$$\sigma = \sigma_\mathrm{N} + \sigma_\mathrm{M} = \frac{N}{\hat{N}}\frac{\hat{w}}{w}\,\hat{\sigma}_\mathrm{N} + \frac{M}{\hat{M}}\left(\frac{\hat{w}}{w}\right)^2 \hat{\sigma}_\mathrm{M} = \frac{P}{\hat{P}}\left(\frac{\hat{w}}{w}\right)^2 \left(\sqrt{1-\Lambda^2}\,\hat{\sigma}_\mathrm{N} + \Lambda\,\hat{\sigma}_\mathrm{M}\right), \tag{16}$$

where P and Λ are the loading parameters introduced in Eq. (2). Quantities with a hat denote parameters and solutions of the reference FE analysis. Respecting the same scaling and boundary conditions for the energy quantities as for the stresses an inverse proportionality of the total energy potential with respect to the Young's modulus is obtained. The strain energy due to normal force loading is scale-invariant with respect to the width. The strain energy under bending loading is inverse proportional to the square of the width. The impact of the Poisson's ratio within the bounds of $0.3 \leq \nu \leq 0.4$ on the potential energy is negligible ($< 0.2\,\%$). Of course the strain energy scales proportionally to the squared loading. In the superposition of the energy quantities the additional coupling term $\Pi^\mathrm{i}_\mathrm{NM} = N\,u_\mathrm{M}$ is present. It corresponds to the work done by the applied normal force N when the subsequently applied bending moment M translates the load application point by u_M. Of course, u_M is zero for symmetric crack configurations. The total strain energy reads

$$\Pi^\mathrm{i} = \Pi^\mathrm{i}_\mathrm{N} + \Pi^\mathrm{i}_\mathrm{M} + \Pi^\mathrm{i}_\mathrm{NM} = \frac{\hat{E}}{E}\left(\left(\frac{N}{\hat{N}}\right)^2 \hat{\Pi}^\mathrm{i}_\mathrm{N} + \left(\frac{M}{\hat{M}}\right)^2 \left(\frac{\hat{w}}{w}\right)^2 \hat{\Pi}^\mathrm{i}_\mathrm{M} + \frac{M}{\hat{M}}\frac{N}{\hat{N}}\frac{\hat{w}}{w}\,\hat{N}\,\hat{u}_\mathrm{M}\right). \tag{17}$$

Using Clapeyron's theorem $\Pi = -\Pi^\mathrm{i}$ and knowing that u_M is zero in the undamaged configurations yields the difference in total potential energy between cracked and uncracked state

$$\Delta\Pi = \frac{\hat{E}}{E}\left(\frac{\hat{w}}{w}\right)^2 \left(\frac{P}{\hat{P}}\right)^2 \left(\left(1-\Lambda^2\right)\Delta\hat{\Pi}_\mathrm{N} + \Lambda^2\,\Delta\hat{\Pi}_\mathrm{M} - 2\sqrt{3}\,\Lambda\sqrt{1-\Lambda^2}\,\frac{\hat{P}}{\hat{w}}\,\hat{u}_\mathrm{M}\right). \tag{18}$$

As Eqs. (16) and (18) show, only the dependence on the hole size and the crack lengths remains undetermined. If all possible parameter configurations are to be investigated a set of about 80 000 linear elastic FEAs for the four non-dimensional parameters ω, $\delta^{(1)}$, $\delta^{(2)}$ and $\delta^{(3)}$ is required. The full analysis was completed within about 48 hours on the standard desktop computer environment used for the present work.

With the stress and energy quantities available an optimization problem is to be solved in order to obtain the failure load and the corresponding finite crack pattern. On any kinematically admissible crack pattern the smallest load needs to be identified satisfying both, the stress and the energy criterion. Using the point method, Eq. (14), the failure load is given by

$$P_\mathrm{f} = \min_{\mathbf{\Delta a}}\left\{\, P \mid \sigma_\mathrm{I}(y) \geq \sigma_\mathrm{c}\ \forall\, y \in \Omega\,(\mathbf{\Delta a}) \ \wedge\ \bar{\mathcal{G}}\,(\mathbf{\Delta a}) \geq \mathcal{G}_\mathrm{c}\right\}. \tag{19}$$

As discussed for Eqs. (8) and (9), only crack patterns including $\Delta a^{(2)}$ are considered. Therefore the solution of the optimization with respect to all possible crack patterns can be split into consecutive steps: First, the minimum failure load with respect to all possible crack lengths $\Delta a^{(2)}$ is determined. In a second step the minimum out of all the loads identified in step one is determined with respect to the crack length ratios ψ_A and ψ_B, cf. Eqs. (8) and (9). The two steps yield the global minimum of the failure load for any possible crack configuration and thus provide the critical load P_f as well as the associated finite crack pattern composed of $\Delta a^{(2)}$ and ψ (either ψ_A or ψ_B). The optimization problem is solved in the same manner for the line method, Eq. (15).

4. Cohesive zone model

Considering the critical loading of open-hole plates, experiments reported in literature cover only special cases like uniaxial tension loading of symmetric structures and thus, symmetric cracking. In order to tackle asymmetric crack onset asymmetric structures or non-uniform loading are necessary. For the present case of non-uniform loading through a combination of tension and bending a cohesive zone model (CZM) in a FE model can be used as a numerical reference solution. A comparison to FFM for arbitrary bending load contributions Λ is possible. A number of studies which report the successful application of CZMs for the prediction of failure loads of for example notches (Gómez

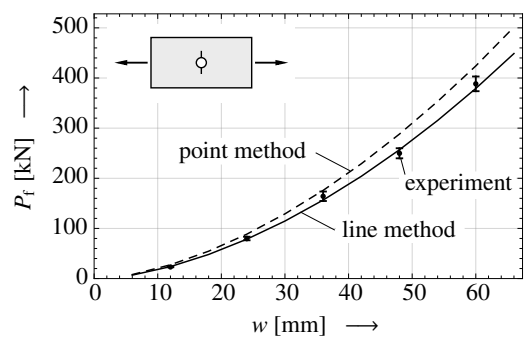

Fig. 4. Comparison of FFM predictions and experimental data (Camanho et al., 2007) in the limit case of uniaxial tension obtained from quasi-isotropic $[90/0/\pm45]_{3s}$ Hexcel IM7/8552 laminate specimens with a hole size of $\omega = 0.167$, $\sigma_c = 845.1$ MPa and $K_{Ic} = 48.0\,\text{MPa}\sqrt{\text{m}}$.

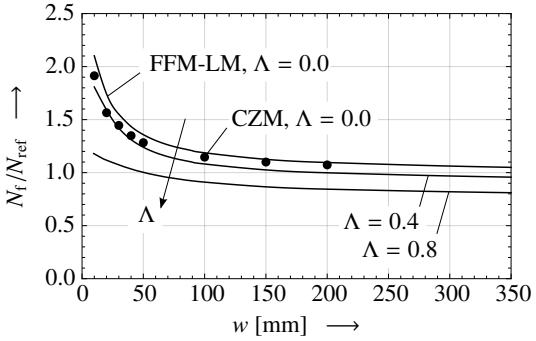

Fig. 5. Rendering of the size effect by the finite fracture mechanics (FFM) and cohesive zone model (CZM) for $\omega = 0.2$ and the same material properties as used in Fig. 4. N_{ref} corresponds to the critical normal force loading for pure strength of materials assessment.

and Elices, 2004) or open-holes (Backlund and Aronsson, 1986; Shin and Wang, 2004) are available in literature. The model combines a stress based damage initiation criterion with an energy based damage evolution law in order to model crack growth along predefined paths. It requires numerical regularization and non-physical parameters such as the cohesive element length. However, good results with respect to the accuracy of predicted failure loads can be obtained.

For the present work, finite thickness cohesive elements from the *Abaqus* element library are placed along the vertical symmetry axis of a full model of the plate (cf. Fig. 1) where the cracks are expected. The structure is loaded until rupture by combination of translational and rotational displacements. A maximum principal stress criterion

$$\frac{\sigma_I}{\sigma_c} = 1\,, \tag{20}$$

is used as the damage initiation criterion. Damage evolution is controlled by a linear degradation of the element stiffness after damage initiation. Cohesive elements are removed from the model when the overall rate of released energy equals the fracture toughness

$$\mathcal{G}_c = \int_0^{\delta_f} \sigma(\delta)\,\mathrm{d}\delta\,, \tag{21}$$

where δ_f denotes the separation at complete debonding and $\mathcal{G}_c$ corresponds to the mode I fracture toughness. Prior to damage initiation $\sigma(\delta)$ represents the continuum element response. After damage initiation $\sigma(\delta)$ is a linearly decreasing function of δ.

The failure load is identified as the peak load in the load-displacement chart. Viscous regularization virtually increases the fracture toughness and can lead to overestimation of the failure load. Thus, the viscous regularization parameter μ is controlled carefully in a parametric convergence study. For the employed regularization parameters $\mu \leq 5 \times 10^{-6}$ the dissipated energy is sufficiently small with respect to the strain energy, $\Pi^{diss} \leq 10^{-3} \times \Pi^{i}$. The, sufficiently accurate failure loads can be expected.

5. Results and discussion

For the limit case of uniaxial tensile loading of open-hole plates experimental results from literature allow for the validation of the presented FFM model. Camanho et al. (2012) report failure loads for open-hole quasi-isotropic Hexcel IM7/8552 laminate specimens. Fig. 4 compares their data to results of the FFM model for both point and line method. Overall the predictions agree well with the experiments. All line method results lie within the margin of error of the specimen tests. Compared to the point method, the line method provides conservative predictions.

Open-holes are well known to exhibit a size effect, i.e. an increased failure load for reduced structural dimensions. It is repeatedly reported in experimental studies, e.g. by Kim et al. (1995) or Li and Zhang (2006). As shown in Fig. 5, the size effect is rendered by both failure models examined in this work. The FFM and CZM predictions agree well

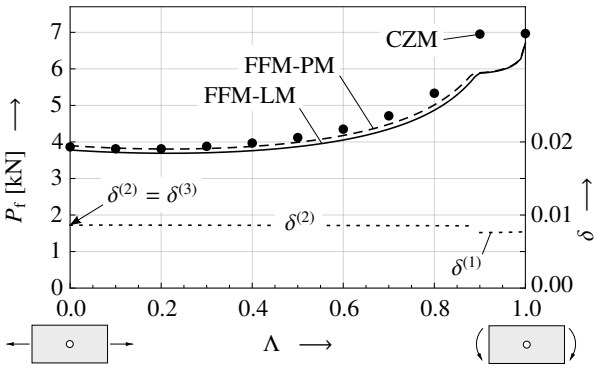

Fig. 6. Failure load predictions by the CZM (dots) and the FFM approach using line method (solid line) and point method (dashed line) with the corresponding finite crack lengths (dotted lines). The material properties $\sigma_c = 100\,\mathrm{MPa}$ and $\mathcal{G}_c = 400\,\mathrm{J/m^2}$ correspond to a polymethyl methacrylate (PMMA). A plate of width $w = 20\,\mathrm{mm}$ and hole size $\omega = 0.2$ is examined.

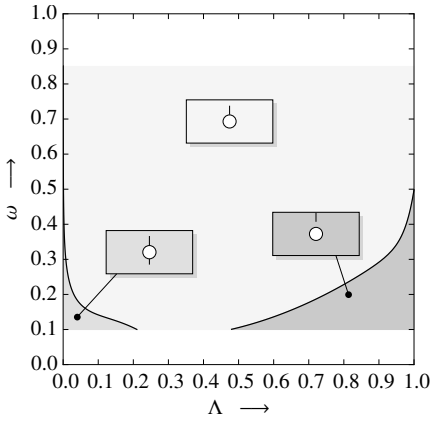

Fig. 7. Crack patterns predicted by finite fracture mechanics depending on the bending load contribution Λ and the relative hole size ω. The data are obtained from a PMMA ($\sigma_c = 113\,\mathrm{MPa}$, $\mathcal{G}_c = 1472\,\mathrm{J/m^2}$) plate of width $w = 5\,\mathrm{mm}$. The ω data is computed in discrete steps in the range $0.1 \le \omega \le 0.85$ and interpolated for the present plot.

in this regard. Fig. 5 also shows that the critical normal force load obviously decreases with increased superimposed bending loading. However, the size effect is observed for any combination of tensile and bending loading.

Fig. 6 shows the FFM failure loads P_f and the associated non-dimensional finite crack lengths $\delta^{(i)}$ as well as the CZM predictions with respect to the amount of bending loading Λ. For uniaxial tension, $\Lambda = 0$, symmetric cracks at the hole $\delta^{(2)} = \delta^{(3)}$ are predicted. With superimposed bending loading a single crack on the bending tension side of the hole $\delta^{(2)}$ is expected to originate. At a critical bending load contribution a transition from the single crack at the hole $\delta^{(2)}$ into a single edge crack on the bending tension side $\delta^{(1)}$ occurs. Here, the failure is bending dominated. The change in observed crack pattern is linked to a kink in the failure load curve. The kink appears for both FFM models as well as for the CZM approach. While FFM and CZM predictions agree well for a wide range of bending load contributions, at $\Lambda = 0.9$ a deviation is apparent because the prediction of the location of the failure load kink differs between the FFM and CZM approaches. For pure bending, $\Lambda = 1.0$, both models are in agreement again.

Fig. 7 shows the dependence of the predicted crack patterns on the amount of bending loading and the hole size. The most dominant failure mode is a single crack at the hole on the bending tension side. Only for comparatively small hole sizes other crack patterns emerge. For small holes and a small bending load contribution cracks of uneven length at the hole are expected. The larger the bending loading the longer the crack on the bending tension side compared to the one on the bending compression side. For uniaxial tensile loading, $\Lambda = 0$, symmetric cracks at the hole are predicted for any hole size ω. At small holes subject to large fractions of superimposed bending a single edge crack on the bending tension side originates. The transition from single crack on the bending tension side of the hole and single edge crack is sudden. No crack configuration involving both these cracks is observed. A crack pattern including all three cracks is only possible at the junction of all three domains. Hence, the simplification of considering only patterns of two cracks introduced in Section 2 is justified. Asymmetric crack patterns are only observed for small structures. Therefore, a plot for a plate of the width $w = 5\,\mathrm{mm}$ is shown. In particular the domain in the bottom left corner of Fig. 7 decreases in size as the width is increased. The used material properties correspond to properties of PMMA (adjusted by Hebel et al. (2010) in order to account for non-linearity effects).

6. Conclusion

The presented finite fracture mechanics model reduces the number of free structural and material parameters describing the open-hole plate subject to combined tensile and in-plane bending loading to only four. The derived closed-form analytical expressions in combination with a numerical parametric study of the remaining four parameters allow for an efficient and comprehensive analysis of crack onset. Critical load predictions of the present model were

found to agree well with experiments and a cohesive zone model. Crack patterns obtained from the finite fracture mechanics model indicate the onset of a single crack emanating from the open-hole on the bending tension side as the most prevalent failure mode. Asymmetric crack patterns are predicted for small holes and a small amount of superimposed bending loading.

References

Andersons, J., Tarasovs, S., Sparninš, E., 2010. Finite fracture mechanics analysis of crack onset at a stress concentration in a UD glass/epoxy composite in off-axis tension. Composites Science and Technology 70, 1380–1385.

Backlund, J., Aronsson, C.G., 1986. Tensile Fracture of Laminates with Holes. Journal of Composite Materials 20, 259–286.

Camanho, P., Erçin, G., Catalanotti, G., Mahdi, S., Linde, P., 2012. A finite fracture mechanics model for the prediction of the open-hole strength of composite laminates. Composites Part A: Applied Science and Manufacturing 43, 1219–1225.

Camanho, P., Maimí, P., Dávila, C., 2007. Prediction of size effects in notched laminates using continuum damage mechanics. Composites Science and Technology 67, 2715–2727.

Carpinteri, A., Cornetti, P., Sapora, A., 2012. A Finite Fracture Mechanics approach to the asymptotic behaviour of U-notched structures. Fatigue and Fracture of Engineering Materials and Structures 35, 451–457.

Carrère, N., Martin, E., Leguillon, D., 2015. Comparison between models based on a coupled criterion for the prediction of the failure of adhesively bonded joints. Engineering Fracture Mechanics 138, 185–201.

Catalanotti, G., Camanho, P., 2013. A semi-analytical method to predict net-tension failure of mechanically fastened joints in composite laminates. Composites Science and Technology 76, 69–76.

Cicero, S., Madrazo, V., Carrascal, I., 2012. Analysis of notch effect in PMMA using the Theory of Critical Distances. Engineering Fracture Mechanics 86, 56–72.

Cornetti, P., Pugno, N., Carpinteri, A., Taylor, D., 2006. Finite fracture mechanics: A coupled stress and energy failure criterion. Engineering Fracture Mechanics 73, 2021–2033.

Erçin, G., Camanho, P., Xavier, J., Catalanotti, G., Mahdi, S., Linde, P., 2013. Size effects on the tensile and compressive failure of notched composite laminates. Composite Structures 96, 736–744.

Gómez, F., Elices, M., 2004. A fracture criterion for blunted V-notched samples. International Journal of Fracture 127, 239–264.

Griffith, A.A., 1921. The Phenomena of Rupture and Flow in Solids. Philosophical Transactions of the Royal Society A: Mathematical, Physical and Engineering Sciences 221, 163–198.

Hebel, J., Becker, W., 2008. Numerical analysis of brittle crack initiation at stress concentrations in composites. Mechanics of Advanced Materials and Structures 15, 410–420.

Hebel, J., Dieringer, R., Becker, W., 2010. Modelling brittle crack formation at geometrical and material discontinuities using a finite fracture mechanics approach. Engineering Fracture Mechanics 77, 3558–3572.

Hell, S., Weißgraeber, P., Felger, J., Becker, W., 2014. A coupled stress and energy criterion for the assessment of crack initiation in single lap joints: A numerical approach. Engineering Fracture Mechanics 117, 112–126.

Kim, J.K., Kim, D.S., Takeda, N., 1995. Notched Strength and Fracture Criterion in Fabric Composite Plates Containing a Circular Hole. Journal of Composite Materials 29, 982–998.

Leguillon, D., 2002. Strength or toughness? A criterion for crack onset at a notch. European Journal of Mechanics – A/Solids 21, 61–72.

Li, J., Zhang, X., 2006. A criterion study for non-singular stress concentrations in brittle or quasi-brittle materials. Engineering Fracture Mechanics 73, 505–523.

Martin, E., Leguillon, D., Carrère, N., 2012. A coupled strength and toughness criterion for the prediction of the open hole tensile strength of a composite plate. International Journal of Solids and Structures 49, 3915–3922.

Romani, R., Bornert, M., Leguillon, D., Le Roy, R., Sab, K., 2015. Detection of crack onset in double cleavage drilled specimens of plaster under compression by digital image correlation – Theoretical predictions based on a coupled criterion. European Journal of Mechanics - A/Solids 51, 172–182.

Shin, C., Wang, C., 2004. An Improved Cohesive Zone Model for Residual Notched Strength Prediction of Composite Laminates with Different Orthotropic Lay-Ups. Journal of Composite Materials 38, 713–736.

Stein, N., Weißgraeber, P., Becker, W., 2015. A model for brittle failure in adhesive lap joints of arbitrary joint configuration. Composite Structures 133, 707–718.

Waddoups, M., Eisenmann, J., Kaminski, B., 1971. Macroscopic Fracture Mechanics of Advanced Composite Materials. Journal of Composite Materials 5, 446–454.

Weißgraeber, P., Becker, W., 2013. Finite Fracture Mechanics model for mixed mode fracture in adhesive joints. International Journal of Solids and Structures 50, 2383–2394.

Weißgraeber, P., Felger, J., Geipel, D., Becker, W., 2015. Cracks at elliptical holes: Stress intensity factor and Finite Fracture Mechanics solution. European Journal of Mechanics - A/Solids 55, 192–198.

Weißgraeber, P., Leguillon, D., Becker, W., 2016. A review of Finite Fracture Mechanics: crack initiation at singular and non-singular stress raisers. Archive of Applied Mechanics 86, 375–401.

Whitney, J., Nuismer, R., 1974. Stress Fracture Criteria for Laminated Composites Containing Stress Concentrations. Journal of Composite Materials 8, 253–265.